# A NEW TIKHONOV REGULARIZATION METHOD

A thesis submitted to the
Kent State University Honors College
in partial fulfillment of the requirements
for University Honors

by
Martin Fuhry
May, 2011

Thesis written by

Martin Fuhry

Approved by

_____, Advisor

_____, Chair, Department of Mathematics

Accepted by

_____, Dean, Honors College

# Table of Contents

**1 Introduction** **1**

**2 The Singular Value Decomposition** **3**

**3 Two Regularization Methods** **7**

3.1 TSVD . . . . . 7

3.2 Tikhonov Regularization . . . . . 10

3.3 The Discrepancy Principle . . . . . 11

3.4 Determining the Regularization Parameter $\mu$ for Tikhonov Regularization . . . . . 13

**4 Proposed Regularization Method** **15**

**5 Computed Examples** **17**

5.1 Phillips . . . . . 19

5.2 Shaw . . . . . 21

5.3 Inverse Laplace . . . . . 23

5.4 Green's Function for the Second Derivative . . . . . 25

5.5 Baart . . . . . 27

5.6 An Optimal Value of $\mu$ . . . . . 29

**6 Conclusions and Future Work** **30**

**7 Bibliography** **31**

# List of Figures


2.1 The singular values from the $200 \times 200$ matrix taken from a discrete ill-posed problem, the Phillips test problem graphed as a function of their index. . . . . 3

2.2 The first six columns of $V$ from the SVD of the $A$ matrix from the Phillips test problem. 4

2.3 The exact and computed solutions to a discrete ill-posed problem. . . . . 6

3.1 The regularized solution to a discrete ill-posed problem. The exact solution is outlined in red and the computed solution to the regularized problem is outlined in dotted blue. 7

3.2 The first five computed solutions for the TSVD of an inverse problem for $k = 1, 2, 3, 4$. The red solid line is the real solution and the dotted lines are the TSVD solutions. . 8

3.3 A graph of $\mu$ versus the difference of $x_\mu$, the computed Tikhonov solution, and $x$, the solution of (1.3). The $\mu$-value determined by the discrepancy principle is marked by a red dot. The optimal $\mu$-value which minimizes the error $||x_{\text{exact}} - x_\mu||$ is marked by a blue dot. . . . . 12

5.1 The computed examples for the Phillips test problem. . . . . 20

5.2 The computed examples for the Shaw test problem. . . . . 22

5.3 The computed examples for the Inverse Laplace test problem. . . . . 24

5.4 The computed examples for the Green's function test problem. . . . . 26

5.5 The computed examples for the Baart test problem. . . . . 28

# List of Tables


1 The relative error in the computed solutions for the Phillips test problem. . . . . 20

2 The relative error in the computed solutions for the Shaw test problem. . . . . 22

3 The relative error in the computed solutions for the Inverse Laplace test problem. . . 24

4 The relative error in the computed solutions for the Deriv2 test problem. . . . . 26

5 The relative error in the computed solutions for the Baart test problem. . . . . 28

6 The relative error in the computed solutions for the Phillips test problem with an optimal $\mu$ regularization parameter. . . . . 29

## Acknowledgements

I would like to thank my mentor Dr. Lothar Reichel for his guidance and encouragement and my defense comittee members, Dr. Eugene Gartland, Dr. Arne Gericke, and Dr. Arden Ruttan.

# 1 Introduction

Even a slight nudge of a telescope can display an entirely different galaxy. Many mathematical models will produce a wildly different output with only a slight change in input. Inverse problems, in particular, frequently exhibit this intense sensitivity to changes in the input. An inverse problem will use a model to reconstruct an input from the corresponding output. For example, the inverse heat equation determines the heat source from a given distribution of heat. These types of inverse problems are extremely sensitive to the initial distributions of the data. So sensitive are these problems, that even minute errors in the data can wildly affect the computed solution.

Many problems in the physical sciences are highly sensitive to changes in their input, including remote sensing, image restoration, medical imaging, astronomy, and inverse heat problems; [1] gives many examples. These mathematical models can be expressed as a linear system of equations such as

$$Ax = b. \tag{1.1}$$

In this system, the matrix $A \in \mathbb{R}^{m \times n}$ with $m \geq n$ describes the model. The input is some vector $x \in \mathbb{R}^n$ and the output is presented in the vector $b \in \mathbb{R}^m$. The inverse problem associated with this model computes the input $x$ given some output $b$ and the known model. We are concerned with computing an approximate solution to the linear least-squares minimization problem associated with the linear system of equations (1.1):

$$\min_{x \in \mathbb{R}^n} ||Ax - b||, \tag{1.2}$$

where the norm $||\cdot||$ is the Euclidean norm. We assume that the solution $x$ is very sensitive to changes in the data $b$. This sensitivity is especially important to consider when error may contaminate the data.

If the available data is not exact, then even a small error may be enough perturb the solution by an enormous amount. Suppose that the available data is contaminated with error; i.e., the available

data can be written as

$$b = \hat{b} + e$$

where the vector $\hat{b}$ is the exact data and the error in the data is represented by the vector $e$. The desired solution $x$ is the solution to the linear system of equations containing the error-free data

$$Ax = \hat{b}. \tag{1.3}$$

Since this problem is so sensitive to changes in the data, even a small error vector may distort the computed solution considerably. The computed solution may be very different from the desired solution and ultimately meaningless.

We are interested in the numerical solutions of these so-called *discrete ill-posed problems*; see [2] for more on discrete ill-posed problems. The solution to these discrete ill-posed problems exhibits the severe sensitivity to errors in the data mentioned. This thesis is concerned with the investigation and development of numerical methods for the solution of discrete ill-posed problems. All discrete ill-posed problems obey the following criteria:

1. The solution is sensitive to perturbations in the data.

2. The singular values of the matrix gradually decay to zero.

The latter is discussed in Section 2.

In order to be able to determine a meaningful approximation of the desired solution of (1.3) from (1.2), the latter problem is first replaced by a nearby problem, where the solution is less sensitive to errors in the data. This replacement is commonly referred to as *regularization*. Tikhonov regularization and regularization by the truncated singular value decomposition (TSVD) are discussed in Section 3. A novel regularization approach combining properties of Tikhonov regularization and TSVD is presented in Section 4. Computed examples that compare the regularization methods discussed can be found in Section 5, and Section 6 contains concluding remarks.

# 2 The Singular Value Decomposition

*Figure 2.1: The singular values from the 200 × 200 matrix taken from a discrete ill-posed problem, the Phillips test problem graphed as a function of their index.*

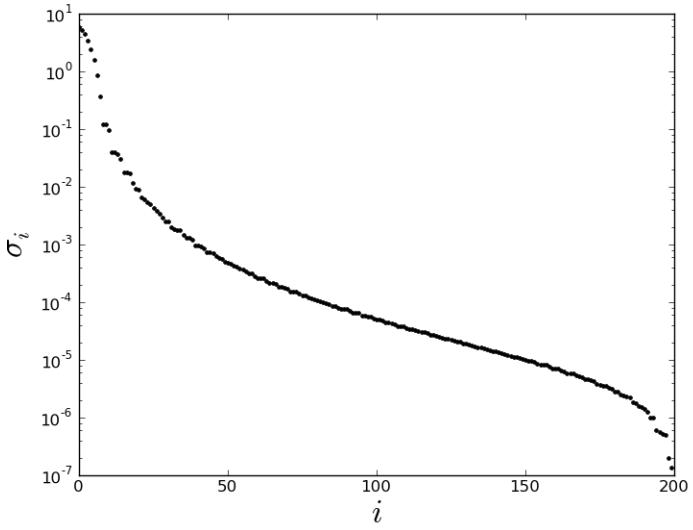


The singular value decomposition (SVD) is a factorization of a matrix, $A$, into

$$A = U\Sigma V^T \tag{2.1}$$

where $U = [u_1, ..., u_m] \in \mathbb{R}^{m\times m}$ is an orthogonal matrix whose columns are the left singular vectors of $A$, and $V = [v_1, ..., v_n] \in \mathbb{R}^{n\times n}$ is an orthogonal matrix whose columns are the right singular vectors of $A$. The nontrivial entries of the diagonal matrix

$$\Sigma = \text{diag}\,[\sigma_1, ..., \sigma_n] \in \mathbb{R}^{m\times n}$$

are the singular values, $\sigma_j$. They satisfy $\sigma_j \geq 0$ and are ordered so that $\sigma_1 \geq \sigma_2 \geq \cdots \geq \sigma_n$. Assume that $A$ has rank $l$. Then, the singular values satisfy $\sigma_1 \geq \sigma_2 \geq \cdots \geq \sigma_l > \sigma_{l+1} = \cdots = \sigma_n = 0$ and

*Figure 2.2: The first six columns of $V$ from the SVD of the $A$ matrix from the Phillips test problem.*

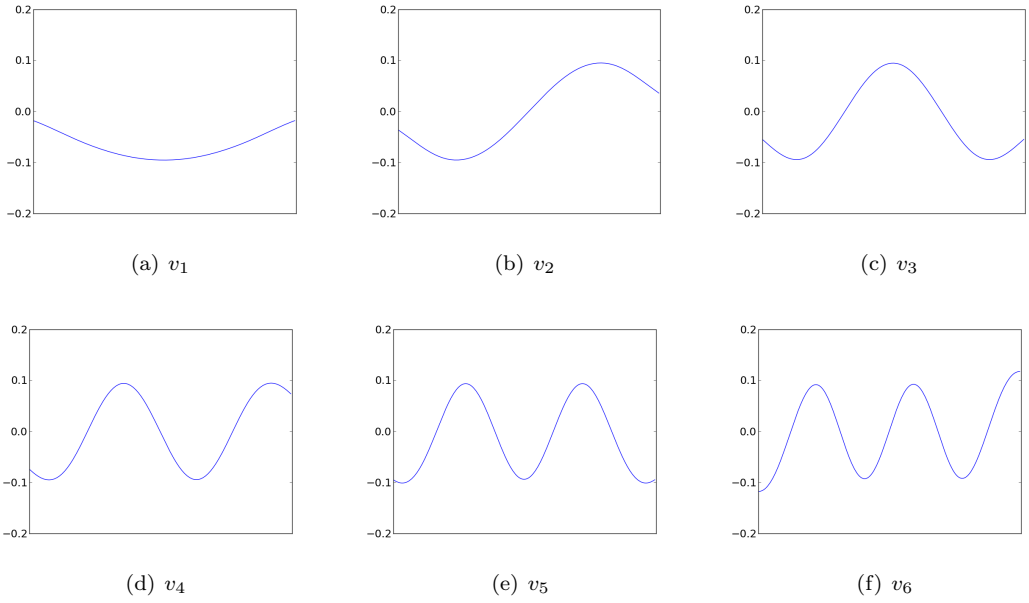

(a) $v_1$ (b) $v_2$ (c) $v_3$

(d) $v_4$ (e) $v_5$ (f) $v_6$

$A$ can be expressed as the sum of $l$ rank-one matrices,

$$A = \sum_{j=1}^{l} \sigma_j u_j v_j^T. \tag{2.2}$$

The most important aspect of the SVD is the singular values, themselves. In discrete ill-posed problems, the singular values of the matrix $A$ decay gradually to zero, as shown in Figure 2.1. These singular values are taken from the matrix $A$ in a discrete ill-posed problem known as the Phillips test problem, further described in the Computed Examples section.

Another important property of the SVD is the nature of the columns of the matrix $V$. Figure 2.2 shows the first six columns of $V$ taken from the SVD of the matrix $A$ in the Phillips test problem. These columns become more oscillatory as we traverse the index. In general, the higher the index of $v_i$, the more oscillatory the vector. This behavior is typical for discrete ill-posed problems.

The columns of $V$ are particularly important when we consider the nature of the given data $b$. In most applications, the exact data, $\hat{b}$, is smooth. The error $e$ in the given data $b$, on the other hand, is typically very erratic. Thus, the first smooth columns of $V$ correlate with the smooth error-free vector $\hat{b}$, while the later oscillatory columns of $V$ correlate with the erratic error $e$.

To give an example of a discrete ill-posed problem, we consider the matrix $A$ in the Phillips

test problem. The decaying singular values of $A$ are shown in Figure 2.1. In this test problem, the solution to the linear least-squares problem (1.2) is very sensitive to changes in the data. To quantify just how sensitive the solution is, we introduce the concept of a *condition number*. The condition number of a matrix $A$ measures the sensitivity of the solution of (1.2) to perturbations in the data. For a rectangular matrix $A$ in $\mathbb{R}^{m\times n}$ of full rank, we define the condition number as the ratio of largest singular value to the smallest nonzero singular value. In this test problem, the condition number of the matrix $A$ is

$$\kappa(A) = \frac{\sigma_1}{\sigma_n} \approx \frac{5.8}{1.4 \cdot 10^{-7}} \approx 4.2 \cdot 10^7.$$

This condition number is rather large, which implies that small perturbations of $b$ may lead to large perturbations in the computed solution $x$. This large condition number, along with the gradual decay of the singular values of $A$, shows that this problem is discrete ill-posed.

Solutions to discrete ill-posed problems are typically useless. Consider the Moore-Penrose pseudoinverse

$$A^\dagger = \sum_{j=1}^{l} \sigma_j^{-1} v_j u_j^T \tag{2.3}$$

of the rank-$l$ matrix (2.2). The solution of minimal Euclidean norm of the least-squares problem (1.2) is given by

$$x = A^\dagger b = A^\dagger(\hat{b} + e) = \hat{x} + A^\dagger e. \tag{2.4}$$

Here $\hat{x}$ is the desired solution of minimal norm of the least-squares problem (1.3) with error-free data vector $\hat{b}$. The error in the solution $x$ in (2.4) caused by the error $e$ in the data $b$ is given by

$$A^\dagger e = \sum_{j=1}^{l} \sigma_j^{-1} v_j u_j^T e.$$

As the index increases, the coefficient $\sigma_j^{-1}$ increases in magnitude. In particular, for discrete ill-posed problems with gradual decay in singular values, the coefficient $\sigma_j^{-1}$ becomes extraordinarily large in magnitude as the index approaches $l$. Additionally, the corresponding vectors $u_j$ become more oscillatory as the index approaches $l$. The ever-increasing magnitude of the coefficients combined

*Figure 2.3: The exact and computed solutions to a discrete ill-posed problem.*

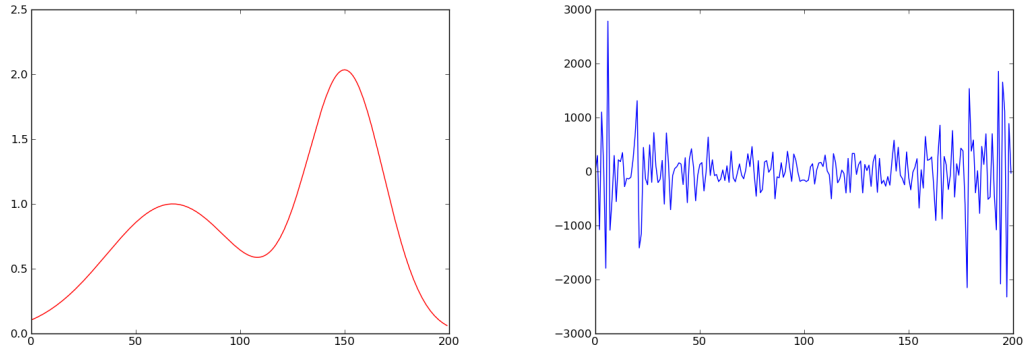


(a) The exact solution to a discrete ill-posed problem.

(b) The computed solution approximated by a least-squares method of least-squares Gaussian elimination.

with the oscillatory nature of the $u_j$ vectors cause the more erratic components of the error vector to dominate. This leaves us with an ultimately useless solution.

Figure 2.3 shows an example of a computation with the different discrete ill-posed problem, Shaw, which is discussed in the Computed Examples section. The norm of the desired solution is only 14, while the solution computed by least-squares Gaussian Elimination has a norm of $8 \cdot 10^3$. Least-squares solutions of discrete ill-posed problems are typically of very large norm, and thus, are meaningless.

In short, we have made two key points, which the reader should keep in mind:

1. Small perturbations of the data may cause large perturbations of the solution.

2. Least-squares solutions of discrete ill-posed problems with error-contaminated data are typically of very large norm and meaningless.

These two key points seem to imply that solving discrete ill-posed systems is a hopeless task to be avoided at all costs.

# 3 Two Regularization Methods

*Figure 3.1: The regularized solution to a discrete ill-posed problem. The exact solution is outlined in red and the computed solution to the regularized problem is outlined in dotted blue.*

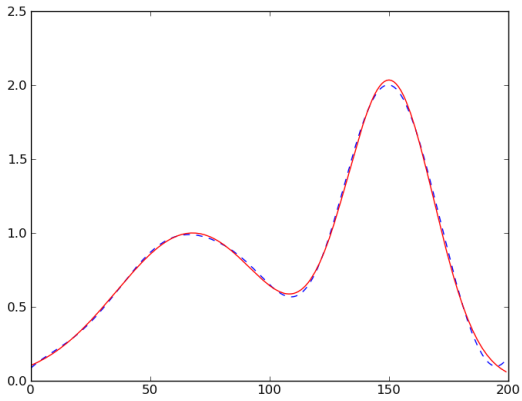


Least-squares solutions of discrete ill-posed problems tend to be of very poor quality, as demonstrated by the previous example. On the other hand, we may be able to obtain very close approximations to the error-free problem's solution by *regularization*, which entails replacing a discrete ill-posed problem with a nearby problem that is no longer discrete ill-posed. Regularization, then, makes the problem less sensitive to small changes in the data.

Recall the least-squares solution of the unregularized discrete ill-posed problem in Figure 2.3. This unregularized solution, computed by Gaussian elimination, was of very large norm and ultimately useless. Figure 3.1 shows the solution of the same discrete ill-posed problem computed by means of a well-known regularization method called the truncated singular value decomposition, discussed below. The next section discusses two types of regularization methods: the truncated singular value decomposition and Tikhonov regularization.

## 3.1 TSVD

We consider the truncated singular value decomposition (TSVD). This regularization method resolves the issue of the problematic tiny positive singular values by setting them to zero. The

*Figure 3.2: The first five computed solutions for the TSVD of an inverse problem for $k = 1, 2, 3, 4$. The red solid line is the real solution and the dotted lines are the TSVD solutions.*

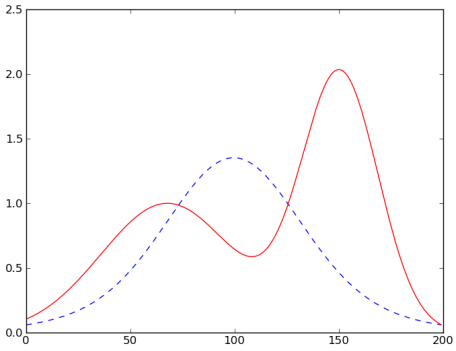


(a) TSVD solution with $k = 1$.

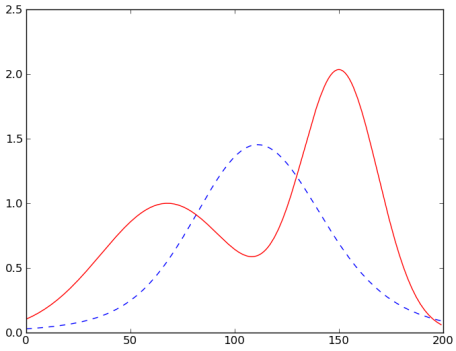


(b) TSVD solution with $k = 2$.

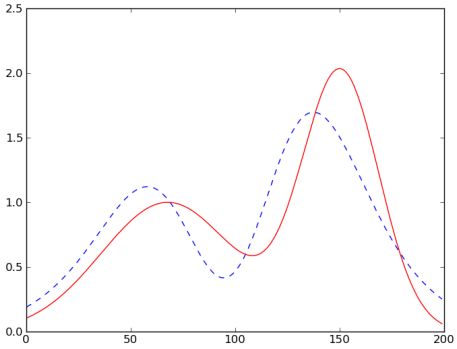


(c) TSVD solution with $k = 3$.

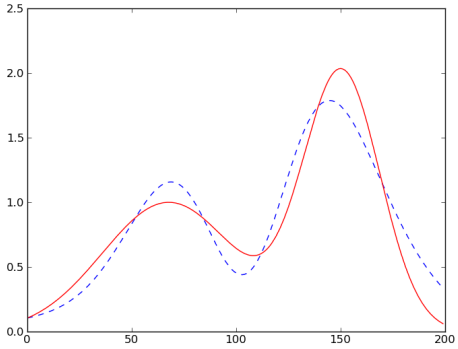


(d) TSVD solution with $k = 4$.

TSVD approximation of $A$ will effectively ignore the smallest singular values. Consider the best rank $k$ approximation of $A$ with respect to the Euclidean norm. It is given by the sum of the first $k$ rank-one matrices in the SVD, i.e.,

$$A_k = \sum_{j=1}^{k} \sigma_j u_j v_j^T. \tag{3.1}$$

In matrix form, (3.1) can be expressed as

$$A_k = U \Sigma_k V^T \tag{3.2}$$

where $\Sigma_k = \text{diag}\,[\sigma_1, ..., \sigma_k, 0, ..., 0]$. The Moore-Penrose pseudo inverse of (3.2) is given by

$$A_k^\dagger = V\Sigma_k^\dagger U^T$$

with

$$\Sigma_k^\dagger = \text{diag}\left[\sigma_1^{-1}, \sigma_2^{-1}, ..., \sigma_k^{-1}, 0, ..., 0\right]$$

for $k \leq l$.

The TSVD method gives the approximate solutions of (1.2) in the form

$$x_k = A_k^\dagger b = V\Sigma_k^\dagger U^T b. \tag{3.3}$$

We can write (3.3) as a linear combination of vectors of $V$:

$$x_k = \sum_{j=1}^{k} \frac{u_j^T b}{\sigma_j} v_j, \qquad k = 1, 2, ..., l. \tag{3.4}$$

Calling $\tilde{x}_k = V^T x_k$ and $\tilde{b} = U^T b$, we first compute

$$x_k = \left[\frac{\tilde{b}_1}{\sigma_1}, \frac{\tilde{b}_2}{\sigma_2}, ... \frac{\tilde{b}_k}{\sigma_k}, 0, ..., 0\right]^T, \qquad k = 1, 2, ..., l.$$

We then evaluate the approximate solution $x_k = V\tilde{x}_k$.

Figure 3.2 shows solutions $x_k$ for $k = 1, 2, 3, 4$. For sufficiently small indexes, as $k$ increases, the computed solution $x_k$ better approximates the actual solution. This is because the first vectors in $V$ amplify the smooth parts of the data without amplifying the noise. When $k$ is too large, the rank-one matrices associated with the larger indices introduce large propogational error into the solution. This will result in a less accurate approximation. The condition number of the matrix $A_k$ provides insight on the nature of choosing the correct $k$.

The TSVD regularizes the problem (1.2) by replacing $A$, which has a large condition number, with a nearby matrix $A_k$, which has a lower condition number for sufficiently small $k$. The condition

number of the rank-$k$ approximation $A_k$ depends entirely on our choice of $k$, i.e.,

$$\kappa(A_k) = \frac{\sigma_1}{\sigma_k}.$$

We can determine how close $A_k$ is to $A$ by considering the norm of the difference

$$||A - A_k|| = ||U\Sigma V^T - U\Sigma_k V^T|| = ||\Sigma - \Sigma_k|| = \sigma_{k+1}.$$

Hence, $\sigma_k$ provides a measure of the distance between $A$ and $A_k$. Choose $k$ too large and the condition number will be large. Conversely, choose $k$ too small, and the resulting matrix $A_k$ will not be a good approximation of the matrix $A$.

## 3.2 Tikhonov Regularization

This regularization method replaces the minimization problem (1.2) by the penalized least squares problem

$$\min_{x \in \mathbb{R}^n} \left\{ ||Ax - b||^2 + ||L_\mu x||^2 \right\}, \tag{3.5}$$

where $L_\mu \in \mathbb{R}^{k \times n}$, $k \leq n$, is called the regularization matrix. The scalar $\mu > 0$ is known as the regularization parameter. The simplest form of Tikhonov regularization takes $L_\mu = \mu I$ for some constant $\mu$. This choice of $L_\mu$ gives us the minimization problem

$$\min_{x \in \mathbb{R}^n} \left\{ ||Ax - b||^2 + \mu^2 ||x||^2 \right\}. \tag{3.6}$$

Least-squares solutions of discrete ill-posed problems tend to give solutions of very large norm, such as the example in Figure 2.3. By penalizing the norm of the solution vector $x$ by weighting it with some positive constant $\mu$, we obtain solutions to (3.6) with smaller norms. These smaller norm solutions can be remarkably accurate approximations of the solution of the error-free problem (1.3).

Choosing $\mu > 0$ guarantees that $A^T A + \mu^2 I$ is invertible. The explicit solution to (3.6) is given by

$$x_\mu = (A^T A + \mu^2 I)^{-1} A^T b. \tag{3.7}$$

When the SVD (2.1) of $A$ is available, we see that the solution vector $x_\mu$ can be expressed as

$$x_\mu = V(\Sigma^T\Sigma + \mu^2 I)^{-1}\Sigma^T\tilde{b}. \tag{3.8}$$

By looking at the SVD, we see that Tikhonov regularization adds a positive constant $\mu^2$ to each singular value $\sigma_i^2$ of $A^TA$. This is referred to as smoothing. Choosing $\mu$ too large is known as oversmoothing, and choosing $\mu$ too small is known as undersmoothing. This smoothing reduces the contributions of each vector $v_i$ to the solution.

The most profoundly affected vectors in $V$ are the ones with highest index, corresponding to those with the highest oscillations and amplitude. This is because of the relative size of the small singular values to the regularization constant $\mu$. When $\sigma_j$ is much larger than $\mu$, adding $\mu^2$ to $\sigma_j^2$ will not have a very profound effect on the magnitude of the sum. On the other hand, very small singular values will be greatly affected by the addition. This smoothing, then, mitigates high frequency components in $\tilde{b}$.

## 3.3 The Discrepancy Principle

When the norm of the error in $b$ is known or can be approximated, we can make use of the *discrepancy principle* [4]. Assuming the norm of the error in $b$ is $||e|| = \epsilon$, the discrepancy principle tells us to choose the regularization parameter so that the residual error of the regularized system is less than or equal to $\eta\epsilon$ for some user-specified constant $\eta > 1$ independent of $\epsilon$.

For TSVD, this means to choose $k$ as small as possible so that

$$||Ax_k - b|| \leq \eta\epsilon. \tag{3.9}$$

For Tikhonov regularization, this means to choose $\mu$ so that

$$||Ax_\mu - b|| = \eta\epsilon. \tag{3.10}$$

Details on how such a value of $\mu$ can be determined inexpensively when the SVD (2.1) is available are discussed in the following subsection.

The discrepancy principle does not provide the optimal solution. In particular, utilizing the discrepancy principle for the Tikhonov regularization problem causes consistent oversmoothing, see

*Figure 3.3: A graph of $\mu$ versus the difference of $x_\mu$, the computed Tikhonov solution, and $x$, the solution of (1.3). The $\mu$-value determined by the discrepancy principle is marked by a red dot. The optimal $\mu$-value which minimizes the error $||x_{exact} - x_\mu||$ is marked by a blue dot.*

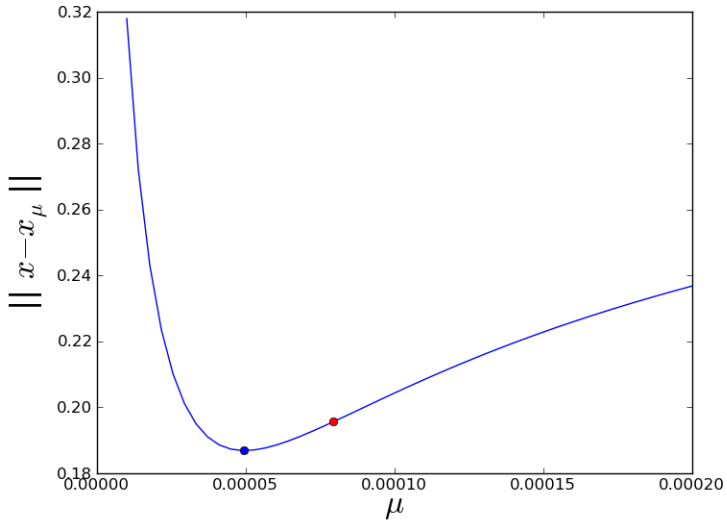


e.g., [5] for a recent discussion. That is, we consistently choose a $\mu$ that is larger than optimal. Figure 3.3 shows the discrepancy principle choose a $\mu$-value which does not exactly solve (1.3). We can see that the red marked $\mu$-value chosen by the discrepancy principle does not minimize the difference between the computed solution $x_\mu$ and the error-free solution $x$. The blue marked $\mu$-value shows that an optimal regularization parameter should be less than the one determined by the discrepancy principle.

For the TSVD, we will use the discrepancy principle to determine the value for the cutoff index in truncation $k$. Utilizing the SVD, we solve (3.9) by choosing $k$ as small as possible so that

$$||\Sigma_k \tilde{x}_k - \tilde{b}|| \leq \eta\epsilon.$$

We detail the method for choosing the best approximation $x_k$ in Algorithm 1.

$A = U\Sigma V^T$
**foreach** $k = 1, ..., n$ **do**
  $\tilde{x}_k = \left[\frac{\tilde{b}}{\sigma_1}, \frac{\tilde{b}}{\sigma_2}, ...\frac{\tilde{b}}{\sigma_k}, 0, ..., 0\right]$
  **if** $||\Sigma_k \tilde{x}_k - \tilde{b}|| \leq \eta\epsilon$ **then**
    Return $x_k = V\tilde{x}_k$
  **end**
**end**

**Algorithm 1**: *Return the solution $x_k$ vector according to the discrepancy principle.*

## 3.4 Determining the Regularization Parameter $\mu$ for Tikhonov Regularization

Define the function

$$\Psi(\mu) = ||Ax_\mu - b||^2 \tag{3.11}$$

The discrepancy principle prescribes that $\mu$ be determined so that

$$\Psi(\mu) = \eta^2\epsilon^2. \tag{3.12}$$

Substituting (3.8) into (3.12) and using the singular value decomposition (2.1) yields the sum

$$\Psi(\mu) = \sum_{j=1}^{n} \left(\frac{\sigma_j^2}{\sigma_j^2 + \mu^2} - 1\right)^2 \tilde{b}_j^2.$$

Introduce the function $\Phi(\nu) = \Psi(1/\mu^2)$, given by

$$\Phi(\nu) = \sum_{j=1}^{n} \frac{\tilde{b}_j^2}{\nu\sigma_j^2 + 1}.$$

It is easy to see that $\Phi$ is decreasing and convex for $\nu \geq 0$. This makes it convenient to solve

$$\Phi(\nu) = \eta^2\epsilon^2 \tag{3.13}$$

by Newton's method, which will converge quadratically and monotonically. The initial iterate is chosen to be $\nu_0 = 0$. The iterations are terminated as soon as $\nu_{k+1} \leq \nu_k$. Newton's method requires

the evaluation of the derivative, which is given by

$$\Phi'(\nu) = \frac{-2\sigma_j^2}{(1+\nu\sigma_j^2)^3}\tilde{b}_j^2.$$

We remark that the function $\Psi(\mu)$ is not guaranteed to be convex. Determining the solution of (3.12) by Newton's method therefore is more complicated than determining the solution of (3.13).

# 4 Proposed Regularization Method

Our proposed regularization method will use properties of both Tikhonov regularization and TSVD. Consider the solution vector $x_\mu$ from (3.8) as the sum

$$x_\mu = \sum_{j=1}^{n} \frac{\sigma_j}{\sigma_j^2 + \mu^2} \tilde{b}_j v_j. \tag{4.1}$$

It follows from (4.1) that Tikhonov regularization dampens every component from $\tilde{b}$. TSVD, on the other hand, does not dampen any components that are not set to zero, as seen in (3.4).

If we knew which solution components contributed the most error to the solution, we could dampen those solution components exclusively. The higher index solution components contain the more oscillatory vectors of $V$. These oscillatory vectors contribute the most error to the solution. Thus, they are precisely the components of the solution that need to be dampened. At the same time, the lower index components do not need to be dampened, as they correspond with the less oscillatory vectors of $V$ and do not contribute much error to the solution. We propose a method which dampens the higher index components of the solution but does not dampen the lower index components.

When $\sigma_j > \mu$, we do not dampen the $j$th solution component. On the other hand, when $\sigma_j \leq \mu$, we replace the dampening $\sigma_j^2 + \mu^2$ denominator in (4.1) with $\mu^2$. Suppose that $\sigma_k > \mu \geq \sigma_{k+1}$. Then, our proposed solution $\bar{x}_\mu$ is given by

$$\bar{x}_\mu = \sum_{j=1}^{k} \sigma_j^{-1} \tilde{b}_j v_j + \sum_{j=k+1}^{n} \frac{\sigma_j}{\mu^2} \tilde{b}_j v_j. \tag{4.2}$$

To see a matrix representation of (4.2), define the matrix

$$P_\mu = \operatorname{diag}\left[\sigma_1^2, \sigma_2^2, \ldots, \sigma_k^2, \mu^2, \ldots, \mu^2\right]. \tag{4.3}$$

Using (4.3), (4.2) can be expressed in matrix form by

$$\bar{x}_\mu = V P_\mu^{-1} \Sigma^T \tilde{b}. \tag{4.4}$$

Our solution (4.4) satisfies

$$(A^T A + L_\mu^T L_\mu)\bar{x}_\mu = A^T b \tag{4.5}$$

for a regularization matrix $L_\mu = D_\mu V^T$ with

$$D_\mu^2 = \text{diag}\left[\max\left\{\mu^2 - \sigma_1^2, 0\right\}, \max\left\{\mu^2 - \sigma_2^2, 0\right\}, ..., \max\left\{\mu^2 - \sigma_n^2, 0\right\}\right]. \tag{4.6}$$

Thus, our proposed method is a modification of Tikhonov regularization that preserves the effects of the lower index solution components while dampening the higher index solution components. The proposed method is summarized by Algorithm 2. The computational complexity of this proposed modification is the same as standard Tikhonov.

1. Determine $\mu$ from Tikhonov regularization using the discrepancy principle.
2. Construct the matrix $P_\mu = \text{diag}\left[\sigma_1^2, ..., \sigma_j^2, \mu^2, ..., \mu^2\right]$ for $\sigma_j > \mu \geq \sigma_{j+1}$.
3. Compute the solution $\bar{x}_\mu = V P_\mu^{-1} \Sigma^T \tilde{b}$.

**Algorithm 2**: *The proposed algorithm for determining* $\bar{x}_\mu$.

# 5 Computed Examples

The following computed examples were performed on an Intel Q6600 Quad Core 64 bit processor running x86_64 Ubuntu Linux 10.10. All tests were performed in the Python programming language using the open source numerical computation modules NumPy and SciPy. Floating point arithmetic was done using 64 bits with machine epsilon roughly equal to $2.2 \cdot 10^{-16}$. The discretization yielded test matrices of size $200 \times 200$. All results are averaged over 1000 tests.

The computed examples themselves were taken from Per Christian Hansen's Regularization Toolset [3] for MATLAB. The examples were imported into Python using Pytave, an open source Python module wrapper for Octave. All code used to generate the tests and run the simulations is available at `http://www.cs.kent.edu/~mfuhry`.

All example problems are derived from the discretization of a Fredholm integral of the first kind, an integral equation of the form

$$\int_a^b K(s,t)f(t)\,dt = g(s). \tag{5.1}$$

In these integral equations, $g(s)$ and $K(s,t)$ are known functions and the integration endpoints $a$ and $b$ are finite or infinite. The goal is to solve for $f(t)$. The discretizations of Fredholm integral equations of the first kind create discrete ill-posed problems. Even a small perturbation in the function $g(s)$ can cause the solution $f(t)$ to be wildly different.

The discretization of (5.1) is done by a quadrature rule and is defined by

$$\int_a^b K(s,t)f(t)dt \approx \sum_{j=1}^{n} K(s,t_j)f(t_j)w_j. \tag{5.2}$$

The $w_j$ values are the weights for the quadrature rule being used. Many problems in Hansen's regularization tools are discretized by the composite midpoint quadrature rule with $w_j = (b-a)/n$ and $t_j = (j - \frac{1}{2})(b-a)/n$. This discretization creates a linear system of equations to be solved for $f(t_j)$.

The computations from each example problem will be presented along with a description of the test problem. We add randomly generated error vectors $e$ to the error-free vector $\hat{b}$. These error

vectors are normally distributed with mean zero and standard deviation scaled so that error vectors have norms of 10%, 5%, 1%, and 0.1% of the norm of the data. Each test is performed 1000 times at each noise level, randomly generating a unique error vector with each iteration. The average residual errors are displayed along with the average graphs for each noise level. We display five significant digits.

We present graphs of the solution vector, as defined in the test problem, and graphs of the solution as determined by the three regularization methods described above: the Tikhonov regularization method, TSVD, and the proposed method. In each graph, the exact solution of the error-free problem is denoted by the solid blue line. The computed solutions are denoted by a red line for the proposed method, a dotted green line for Tikhonov regularization, and a dash-dotted blue line for TSVD. Finally, we present tables comparing the relative error in the computed solution. Let $x_{\text{exact}}$ be the error-free solution and $x_{\text{computed}}$ be the computed solution from each regularization method. For each noise level, we present the relative difference between the error-free solution and the computed solution:

$$||x_{\text{computed}} - x_{\text{exact}}||/||x_{\text{exact}}||.$$

## 5.1 Phillips

The Phillips test problem is a discretization of a Fredholm integral equation of the first kind. We define the function $\phi(x)$ as

$$\phi(x) = \begin{cases} 1 + \cos(\frac{\pi x}{3}), & |x| < 3 \\ 0, & |x| \geq 3 \end{cases}.$$

Define the kernel $K(s,t)$ and the solution $f(x)$ as

$$\begin{aligned} K(s,t) &= \phi(s-t), \\ f(t) &= \phi(t), \\ g(s) &= (6-|s|)\left(1 + \frac{1}{2}\cos\left(\frac{\pi s}{3}\right)\right) + \frac{9}{2\pi}\sin\left(\frac{\pi|s|}{3}\right). \end{aligned}$$

Our integration intervals are $[-6, 6]$.

*Figure 5.1: The computed examples for the Phillips test problem.*

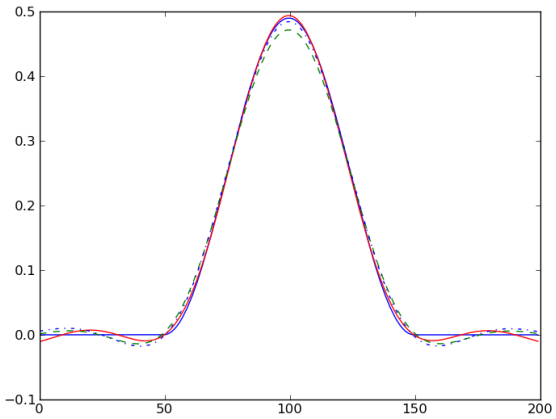


(a) Phillips test problem with 10.0% noise.

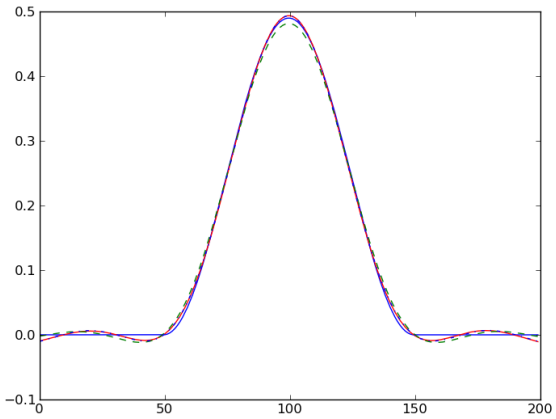


(b) Phillips test problem with 5.0% noise.

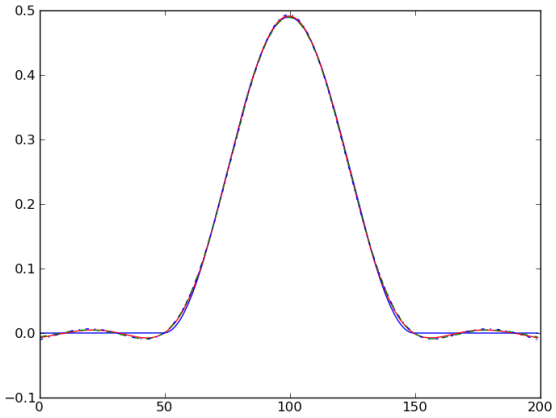


(c) Phillips test problem with 1.0% noise.

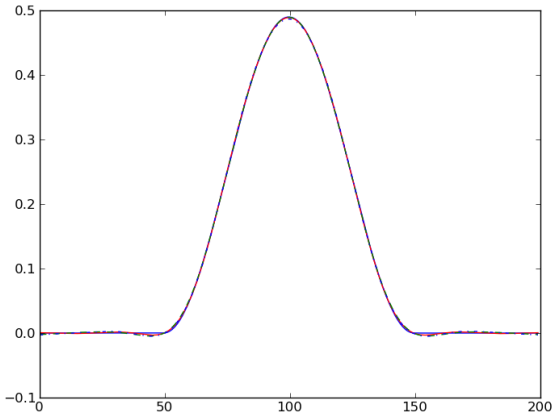


(d) Phillips test problem with 0.1% noise.

*Table 1: The relative error in the computed solutions for the Phillips test problem.*

| **Noise Level** | **Proposed** | **Tikhonov** | **TSVD** |
|---|---|---|---|
| 10.0% | $2.4005 \cdot 10^{-2}$ | $5.0917 \cdot 10^{-2}$ | $4.3606 \cdot 10^{-2}$ |
| 5.0% | $2.3171 \cdot 10^{-2}$ | $3.4606 \cdot 10^{-2}$ | $2.4826 \cdot 10^{-2}$ |
| 1.0% | $1.7678 \cdot 10^{-2}$ | $2.0641 \cdot 10^{-2}$ | $2.4311 \cdot 10^{-2}$ |
| 0.1% | $5.6966 \cdot 10^{-3}$ | $8.5855 \cdot 10^{-3}$ | $9.9050 \cdot 10^{-3}$ |

## 5.2 Shaw

Image restoration problems are typical real world examples of discrete ill-posed problems. The Shaw test problem is an example of a one-dimensional image restoration problem. The kernel function $K$ and the solution function $f$ are given by,

$$K(s,t) = (\cos(s) + \cot(t))^2 \left( \frac{\sin(u)}{u} \right)^2,$$

$$\text{with } u = \pi(\sin(s) + \sin(t)),$$

$$f(t) = a_1 \exp(-c_1(t - t_1)^2) + a_2 \exp(-c_2(t - t_2)^2).$$

In Hansen's implementation, the parameters are given as $a_1 = 2, a_2 = 1, c_1 = 6, c_2 = 2, t_1 = 0.8, t_2 = -0.5$. These parameters give the solution vector two distinctive peaks. We use the integration interval $[-\pi/2, \pi/2]$.

*Figure 5.2: The computed examples for the Shaw test problem.*

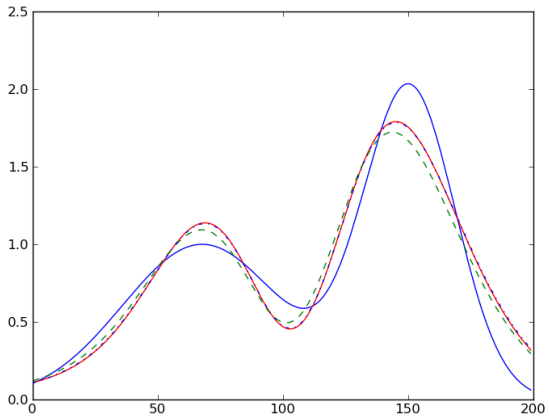


(a) Shaw test problem with 10.0% noise.

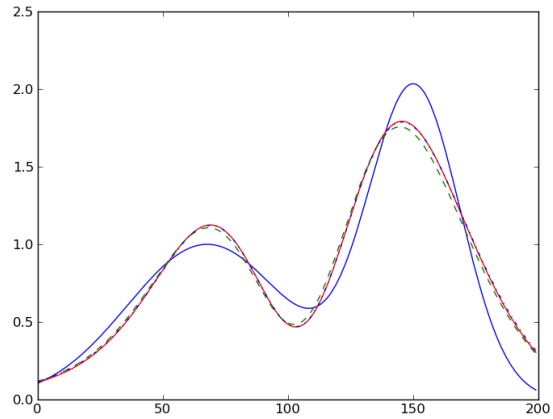


(b) Shaw test problem with 5.0% noise.

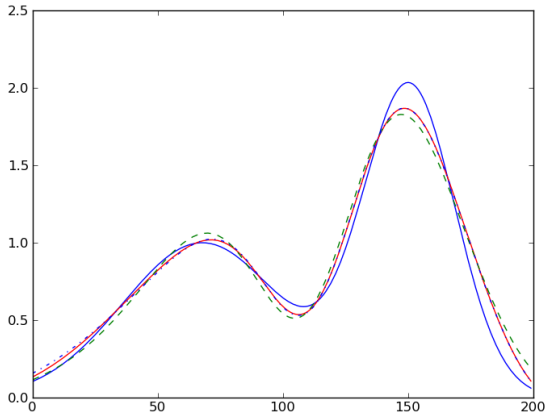


(c) Shaw test problem with 1.0% noise.

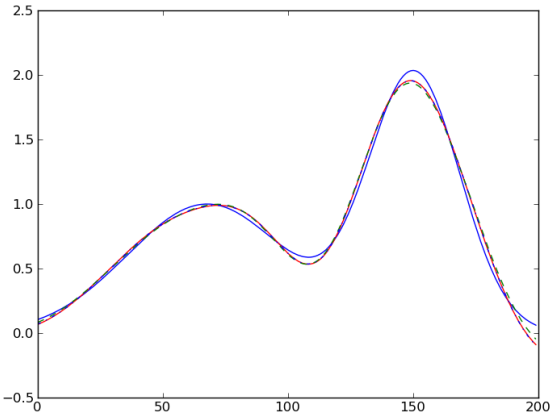


(d) Shaw test problem with 0.1% noise.

*Table 2: The relative error in the computed solutions for the Shaw test problem.*

| **Noise Level** | **Proposed** | **Tikhonov** | **TSVD** |
|---|---|---|---|
| 10.0% | $1.6040 \cdot 10^{-1}$ | $1.6959 \cdot 10^{-1}$ | $1.6167 \cdot 10^{-1}$ |
| 5.0% | $1.5263 \cdot 10^{-1}$ | $1.5777 \cdot 10^{-1}$ | $1.5465 \cdot 10^{-1}$ |
| 1.0% | $8.4161 \cdot 10^{-2}$ | $1.0979 \cdot 10^{-1}$ | $8.5914 \cdot 10^{-2}$ |
| 0.1% | $4.6811 \cdot 10^{-2}$ | $4.9230 \cdot 10^{-2}$ | $4.7207 \cdot 10^{-2}$ |

## 5.3 Inverse Laplace

The inverse Laplace test problem is a discretization of the inverse Laplace transformation by using a Gauss-Laguerre quadrature. The kernel is given by

$$K(s,t) = e^{-st}$$

and the integration intervals are $[0, \infty)$. Of the four implemented variations of this problem in Hansen's regularization tools, we use the solution $f$ right-hand side $g$ given by

$$f(t) = e^{-t/2},$$
$$g(s) = \frac{1}{s + 1/2}.$$

*Figure 5.3: The computed examples for the Inverse Laplace test problem.*

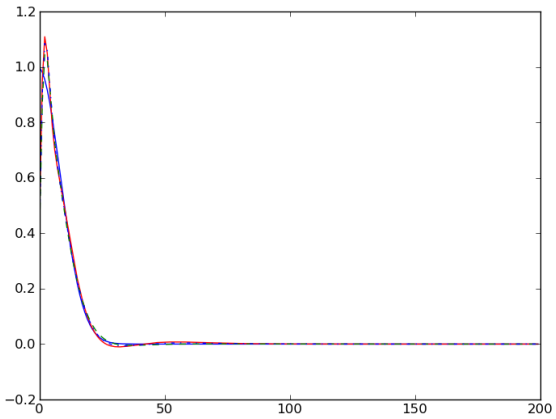


(a) Inverse Laplace test problem with 10.0% noise.

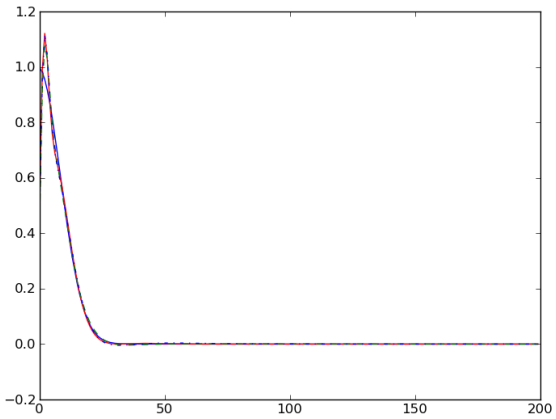


(b) Inverse Laplace test problem with 5.0% noise.

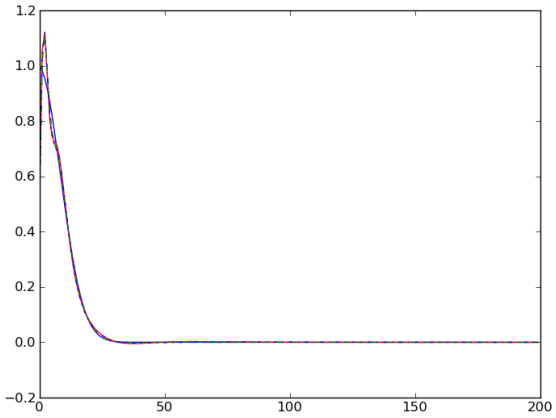


(c) Inverse Laplace test problem with 1.0% noise.

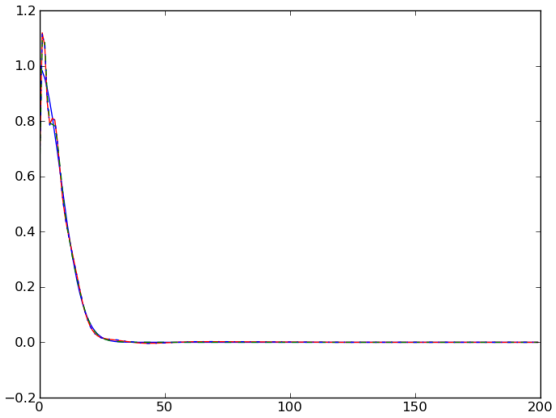


(d) Inverse Laplace test problem with 0.1% noise.

*Table 3: The relative error in the computed solutions for the Inverse Laplace test problem.*

| **Noise Level** | **Proposed** | **Tikhonov** | **TSVD** |
|---|---|---|---|
| 10.0% | $2.0299 \cdot 10^{-1}$ | $2.1438 \cdot 10^{-1}$ | $2.1301 \cdot 10^{-1}$ |
| 5.0% | $1.9185 \cdot 10^{-1}$ | $2.0232 \cdot 10^{-1}$ | $1.9930 \cdot 10^{-1}$ |
| 1.0% | $1.7253 \cdot 10^{-1}$ | $1.7831 \cdot 10^{-1}$ | $1.7710 \cdot 10^{-1}$ |
| 0.1% | $1.4652 \cdot 10^{-1}$ | $1.5055 \cdot 10^{-1}$ | $1.4869 \cdot 10^{-1}$ |

## 5.4 Green's Function for the Second Derivative

This test problem, which we will refer to as the Deriv2 test problem, is a second derivative problem with the kernel $K$ given as the Green's function for the second derivative.

$$K(s,t) = \begin{cases} s(t-1), & s < t \\ t(s-1), & s \geq t \end{cases}.$$

The solution $f$ and right-hand side $g$ are given by

$$f(t) = t,$$
$$g(s) = \frac{s^3 - s}{6},$$

with integration intervals [0,1].

*Figure 5.4: The computed examples for the Green's function test problem.*

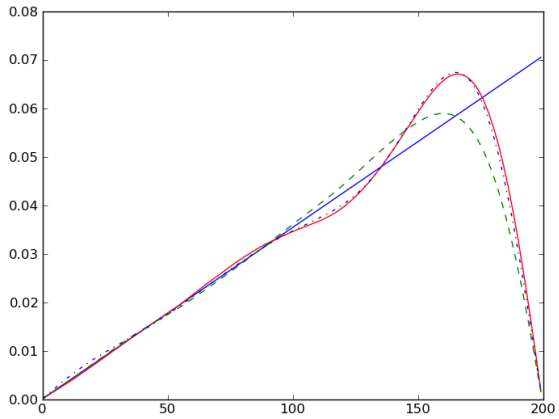


(a) Deriv2 test problem with 10.0% noise.

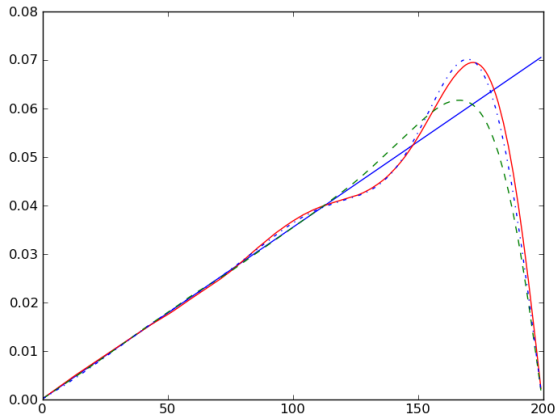


(b) Deriv2 test problem with 5.0% noise.

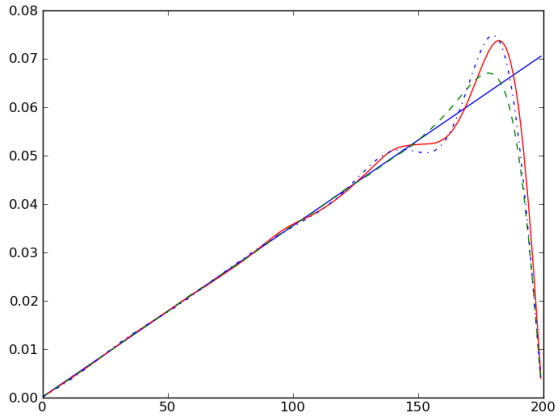


(c) Deriv2 test problem with 1.0% noise.

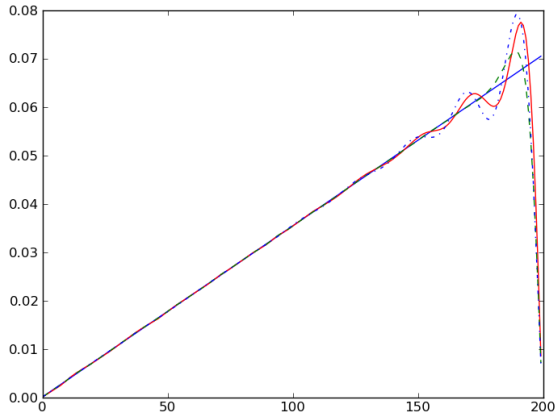


(d) Deriv2 test problem with 0.1% noise.

*Table 4: The relative error in the computed solutions for the Deriv2 test problem.*

| **Noise Level** | **Proposed** | **Tikhonov** | **TSVD** |
|---|---|---|---|
| 10.0% | $3.1601 \cdot 10^{-1}$ | $3.4620 \cdot 10^{-1}$ | $3.2709 \cdot 10^{-1}$ |
| 5.0% | $2.8449 \cdot 10^{-1}$ | $3.1081 \cdot 10^{-1}$ | $3.0264 \cdot 10^{-1}$ |
| 1.0% | $2.2051 \cdot 10^{-1}$ | $2.4009 \cdot 10^{-1}$ | $2.4318 \cdot 10^{-1}$ |
| 0.1% | $1.5103 \cdot 10^{-1}$ | $1.6388 \cdot 10^{-1}$ | $1.7204 \cdot 10^{-1}$ |

## 5.5 Baart

The Baart test problem has a kernel

$$K(s,t) = \exp(s\cos(t)).$$

The right-hand side $g$ is given by

$$g(s) = 2\frac{\sin(s)}{s}.$$

The solution $f$ is

$$f(t) = \sin(t).$$

The integration intervals are $[0, \pi/2]$ for $s$ and $[0, \pi]$ for $t$.

*Figure 5.5: The computed examples for the Baart test problem.*

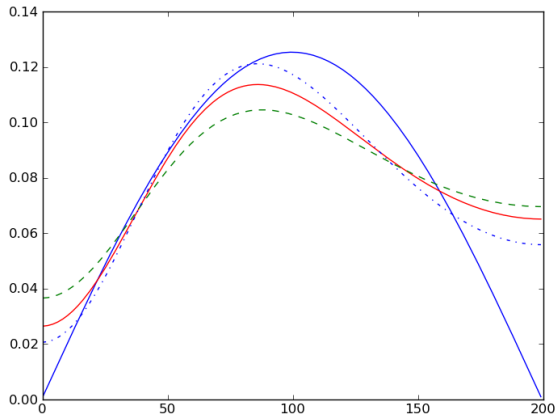


(a) Baart test problem with 10.0% noise.

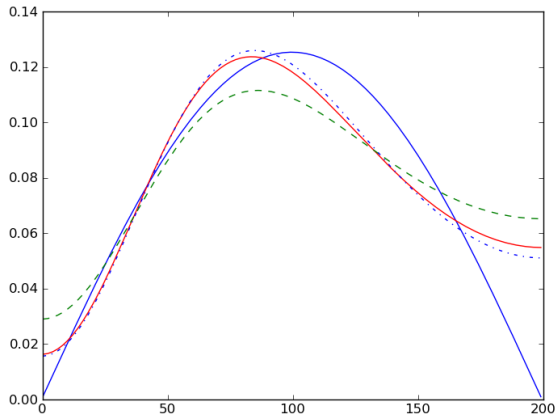


(b) Baart test problem with 5.0% noise.

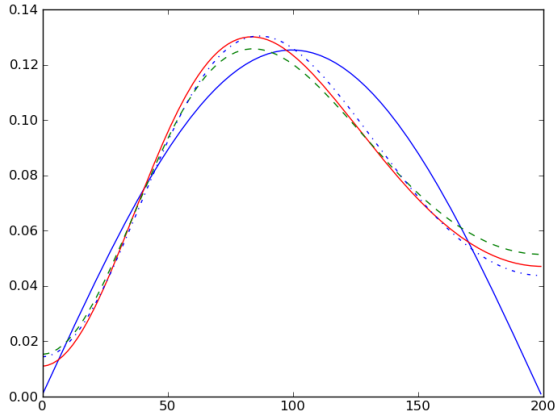


(c) Baart test problem with 1.0% noise.

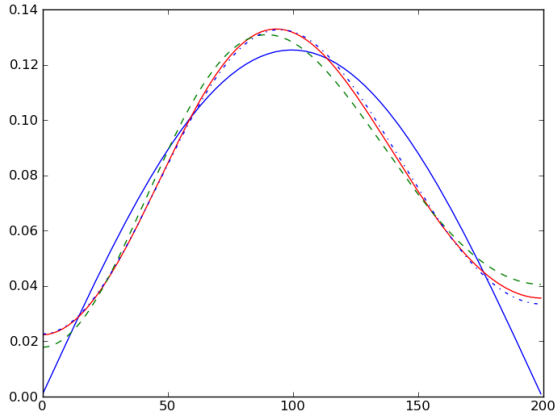


(d) Baart test problem with 0.1% noise.

*Table 5: The relative error in the computed solutions for the Baart test problem.*

| **Noise Level** | **Proposed** | **Tikhonov** | **TSVD** |
|---|---|---|---|
| 10.0% | $2.1409 \cdot 10^{-1}$ | $2.5804 \cdot 10^{-1}$ | $1.7293 \cdot 10^{-1}$ |
| 5.0% | $1.7347 \cdot 10^{-1}$ | $2.2126 \cdot 10^{-1}$ | $1.6035 \cdot 10^{-1}$ |
| 1.0% | $1.5868 \cdot 10^{-1}$ | $1.6330 \cdot 10^{-1}$ | $1.4154 \cdot 10^{-1}$ |
| 0.1% | $1.1531 \cdot 10^{-1}$ | $1.2701 \cdot 10^{-1}$ | $1.0761 \cdot 10^{-1}$ |

## 5.6 An Optimal Value of $\mu$

As shown in Figure 3.3, the discrepancy principle consistently oversmooths the computed solutions. The optimal $\mu$ value minimizes the error between the computed solution $x_\mu$ and the true solution $x$. In the following example, we numerically estimate the optimal value of $\mu$ by using the error free solution. To obtain our optimal value of $\mu$, we choose $\mu$ so that the error between the computed solution and actual solution is minimized. We do not use the discrepancy principle; we use the actual error-free solution to decide $\mu$.

We chose the Phillips test problem as our example and averaged the results over 1000 iterations with matrices of size 200×200. Table 6 shows the relative error in the computed solution with the approximate optimal $\mu$ value chosen as the regularization parameter. Even without the discrepancy principle, our proposed regularization method consistently outperforms Tikhonov regularization.

*Table 6: The relative error in the computed solutions for the Phillips test problem with an optimal $\mu$ regularization parameter.*

| **Noise Level** | **Proposed** | **Tikhonov** | **TSVD** |
|---|---|---|---|
| 10.0% | $2.3270 \cdot 10^{-2}$ | $4.3913 \cdot 10^{-2}$ | $4.2695 \cdot 10^{-2}$ |
| 5.0% | $2.1570 \cdot 10^{-2}$ | $3.1657 \cdot 10^{-2}$ | $2.4883 \cdot 10^{-2}$ |
| 1.0% | $1.5704 \cdot 10^{-2}$ | $1.9239 \cdot 10^{-2}$ | $2.3876 \cdot 10^{-2}$ |
| 0.1% | $5.4651 \cdot 10^{-3}$ | $8.1937 \cdot 10^{-3}$ | $9.9236 \cdot 10^{-3}$ |

# 6 Conclusions and Future Work

In every test, our method outperforms Tikhonov regularization in terms of relative error in the computed solution. Graphically, the solutions from our method look at least as good as the solutions from Tikhonov regularization and TSVD. While the tests displayed are averaged over 1000 iterations, under certain conditions, the competing Tikhonov regularization and TSVD methods were able to outperform our proposed method. The Baart test, in particular, manifests this behavior; indeed, the TSVD method slightly outperforms the proposed method in every noise level. Furthermore, at times, this method displayed only modest improvements over the competing methods of regularization, most notably in the Inverse Laplace test problem. Nonetheless, the improvement over Tikhonov is consistent overall, and improvements over TSVD are fairly consistent. Current implementations of Tikhonov regularization could certainly switch to using our proposed method to gain a definite improvement, albeit small.

# 7 Bibliography


[1] Groetsch, Charles W. *Inverse Problems in the Mathematical Sciences*. Braunschweig/Wiesbaden: Bertelsmann Publishing Group International, 1993.

[2] Hansen, P.C. *Rank-Deficient and Discrete Ill-Posed Problems*. Philadelphia: SIAM, 1998.

[3] Hansen, P.C. *Regularization tools version 4.0 for Matlab 7.3*. SIAM Numerical Algorithms, 46, pp. 189-194, 2007.

[4] Morozov, V. A. *On the solution of functional equations by the method of regularization*. Soviet Math. Dokl., 7, pp. 414-417, 1966.

[5] Klann, E. and Ramlau, R. *Regularization by fractional filter methods and data smoothing*. Inverse Problems, 24, 2008.

[6] Groetsch, Charles W. *The Theory of Tikhonov Regularization for Fredholm Equations of the First Kind*. Pitman: Boston, 1984.

[7] Trefethen, Lloyd N. and Bau, David III. *Numerical Linear Algebra*. Philadelphia: SIAM, 1997.

[8] J. M. Varah. *On the numerical solution of ill-conditioned linear systems with applications to ill-posed problems*. Philadelphia: SIAM J. Numer. Anal., 10, pp. 257-267, 1973.

[9] L. Reichel and H. Sadok *A new L-curve for ill-posed problems*. J. Comput. Appl. Math., 219, pp. 493-508, 2008.

[10] S. Morigi, L. Reichel, and F. Sgallari, *A truncated projected SVD method for linear discrete ill-posed problems*. Numer. Algorithms, 43, pp. 197-213, 2006.